GeoConvention 2014
FOCUS
adapt
refine
sustain

Where does the proppant go? Examining the application of electromagnetic methods for hydraulic fracture characterization

Lindsey J. Heagy and Douglas W. Oldenburg
Geophysical Inversion Facility, University of British Columbia
Vancouver, British Columbia

Jiuping Chen
Schlumberger Technology Corporation
Richmond, California

Summary

Hydraulic fracturing has allowed hydrocarbon exploration and production to expand to shales and tight formations and this has changed the way a drilling target is defined. Fracturing is used to create pathways for the resource to flow from shales and tight formations to the well bore, where it can be produced. Despite advances in the technology, there are still unknowns in the process. One of the main unknowns is the distribution of proppant, which keeps the fracture pathways open. Here we investigate the potential of introducing highly conductive particles into the proppant and imaging the location of the proppant using electromagnetic surveys. Simulating expected responses, and thus determining if the technique is viable, requires upscaling the physical property structure from a millimeter scale to a meter scale. Maxwell's electromagnetic equations are then solved on a reservoir scale. Results indicate that signal well above the expected noise level should be obtained with current transmitter and receiver technology.

Introduction

Hydraulic fracturing has changed and continues to impact exploration and production of hydrocarbons in Canada and around the world. It is used to create pathways for hydrocarbons to flow in low permeability formations. As a result, hydraulic fracturing has created a way to access resource from environments where this previously would have been unrealistic.

A fracture can be induced in a formation by pumping fluid under high pressure into a segment of a well. To keep the fractures open, sand or ceramic particles, referred to as proppant, are pumped into the newly created fractures. The extent of the fracture and distribution of proppant within the reservoir are significant factors influencing the resulting production from the reservoir (King, 2010; Britt et al., 2006; Cipolla and Wright, 2000).

Despite recent advances, there are still many unknowns; chief among them is the extent and distribution of proppant within the reservoir. Existing technologies such as microseismic and tiltmeters, monitor the acoustic events created during the fracture propagation and the ground deformation due to the presence of a fracture, respectively. However, neither of these contains information about the proppant. Well logs and tracers are used to monitor fluid distribution and fracture orientation but are limited in their depth of investigation to within a few meters of the well bore. To

delineate the extent of the proppant within the reservoir, we need a method that is both sensitive to the presence of proppant and can be implemented on the reservoir scale (Cipolla and Wright, 2000; Warpinski, 1996; Barree et al., 2002; Cipolla et al., 2009).

To accomplish this task, we propose to use electromagnetic geophysical techniques (EM). For EM to be a valuable technique for imaging a hydraulic fracture, we require that the fracture have physical properties (ie. electrical conductivity, magnetic permeability, or dielectric permittivity) which are distinct from the host reservoir rock. We also require that the survey be designed so that it excites and detects this contrast. We have some control over the physical properties of the proppant, since it is a material we pump into the ground. By creating an electrically conductive proppant, for instance by coating it with graphite, or creating a magnetic proppant by including minerals such as magnetite, the propped fracture can be made distinct from the host reservoir. This provides a geophysical target we aim to characterize.

Overview of Physical Properties

The materials currently used as proppant, typically sand and ceramics, tend to have similar physical properties to the reservoir that they are being pumped into, making it difficult to detect them on the scale of the reservoir. However, if the proppant were made electrically conductive, for instance by coating it with graphite, it may create a sufficient physical property contrast that can be imaged using EM.

To investigate this, we begin with numerical modelling. A propped fracture presents a challenging problem because of its scaling. The proppant particles have scale lengths on the order of microns to millimeters; fractures tend to have a width on the order of millimeters, but can extend tens of meters in height and hundreds of meters laterally. The challenge numerically is that we must capture the affects of the fine scale physical property variations, while being able to model a domain that includes the extent of the fracture. Simply applying a mesh that captures the fine-scale variations will typically lead to a mesh that is too large to work with. We require a method of assigning effective physical properties on a meter-scale that we can work with computationally.

Two broad categories of methods can accomplish this: analytical methods, for instance, where we approximate the fracture as a collection of ellipsoids filled with proppant and fluid (Berryman and Hoversten, 2013; Shafiro and Kachanov, 2000) and numerical methods, where we solve an inverse problem for the effective properties (Durlofsky, 2003). To demonstrate, we develop an example using the analytical approach.

Assigning Physical Properties to a Fractured Reservoir

The fracture model is treated in two stages, conceptually demonstrated in Figure 1. First, we estimate the effective conductivity of a mixture of proppant and fluid, σ_2. Next, we assume that the fracture can be thought of as consisting of a collection of aligned ellipsoids, filled with a mixture of proppant and fluid. The ellipsoids may be aligned in a single or multiple directions. With this assumption, the effective conductivity of a fractured volume of rock can be assigned. In both cases, we use the self-consistent effective medium theory (Bruggeman, 1935), namely

$$\sum_{j=1}^{N} \phi_j \left(\mathbf{\Sigma}^* - \sigma_j \mathbf{I} \right) \mathbf{R}^{(j,*)} = 0 \tag{1}$$

where N is the number of different phases of materials, ϕ_j is the volume fraction of the j-th phase, and σ_j is the electrical conductivity of the j-th phase. $\mathbf{\Sigma}^*$ is the 3×3 effective conductivity tensor, and $\mathbf{I}$ is the 3×3 identity matrix. The matrix $\mathbf{R}^{(j,*)}$ is the electric field concentration tensor, and depends both on the shape of the inclusions (ie. proppant particles or cracks composing a fracture) and conductivity of the j-th phase, as well as the effective conductivity $\mathbf{\Sigma}^*$. To solve for the effective conductivity, which is an implicit expression, we choose an initial guess and update that guess until the recovered effective conductivity converges within a pre-defined tolerance.

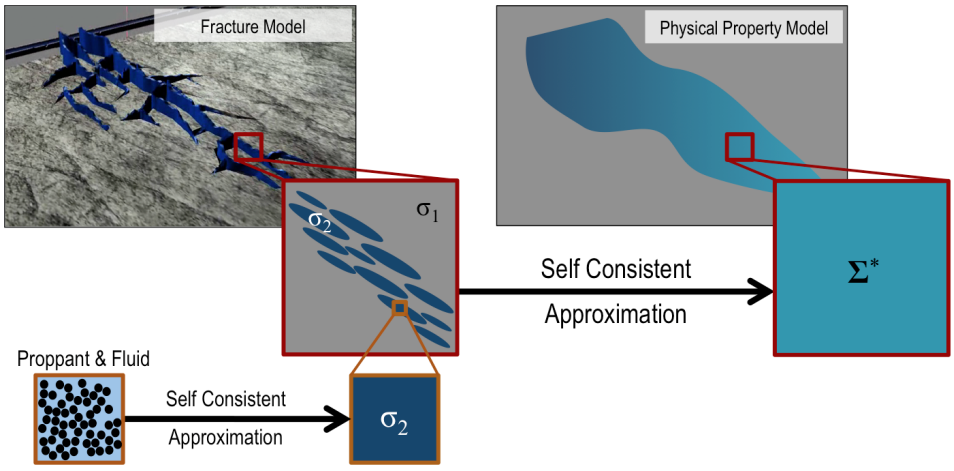

Figure 1: Two stage process of applying effective medium theory to create an effective conductivity model of a fractured volume of rock. We assume that the fracture is composed of ellipsoidal cracks which contain proppant and fluid. The proppant-fluid mixture has an effective conductivity σ_2, which depends on the conductivity of the fluid and proppant particles, as well as their relative concentrations. We approximate a fractured volume of rock as being composed of collections of aligned ellipsoids. Effective medium theory is then applied to create an effective conductivity model of the fractured reservoir, $\boldsymbol{\Sigma}^*$

Assigning Effective Properties of a Proppant-Fluid Mixture

First, the properties of the material filling the fractures is examined. We assume a mixture composed of two materials, fluid and proppant, and that the proppant particles are approximately spherical. To solve for the effective conductivity, we invoke equation 1, where, for a material composed of spherical inclusions,

$$\mathbf{R}^{(j,*)} = \left[\mathbf{I} + \frac{1}{3}\boldsymbol{\Sigma}^{*-1}(\sigma_j \mathbf{I} - \boldsymbol{\Sigma}^*)\right]^{-1}. \tag{2}$$

In this case, the tensor-values in equation 1 reduce to scalars, and the resulting effective conductivity is isotropic (depicted as σ_2 in Figure 1). To demonstrate the results of this method, we examine 5 different mixtures where the values of the electrical conductivity of the proppant range logarithmically from 10 S/m to 10^5 S/m. The upper range of the conductivities, 10^4 to 10^5 S/m, is consistent with the conductivity of graphite. The fluid we consider has an electrical conductivity of 3 S/m, similar to that of seawater. Figure 2 shows the calculated effective conductivities of the 5 different proppant-fluid mixtures as the volume fraction of proppant in the mixture is varied. At low volume concentrations of proppant, the conductivity of the particles has little impact on the resulting effective conductivity of the mixture. However, once the proppant comprises more than $1/3$ of the volume of the mixture, the conductivity of the proppant significantly affects the resulting effective conductivity. This is the *percolation effect*, where statistically it is likely that the particles are at a high enough concentration to touch, forming connected, electrically conductive pathways (cf. Torquato (2002)).

Assigning Effective Properties of Fractured Rock Volume

Now that we have determined the properties of the material filling the fracture, we aim to assign properties to a fractured volume of rock. The propped region of the fracture is approximated as a collection of ellipsoids, filled with the proppant-fluid mixture. For a material composed of ellipsoidal inclusions, the factor of $1/3$ in equation 2 is replaced with the corresponding depolarization tensor that depends on the semi-axes of the ellipsoids (cf. Shafiro and Kachanov (2000)). In the case of aligned ellipsoids, the resulting effective conductivity model will be anisotropic.

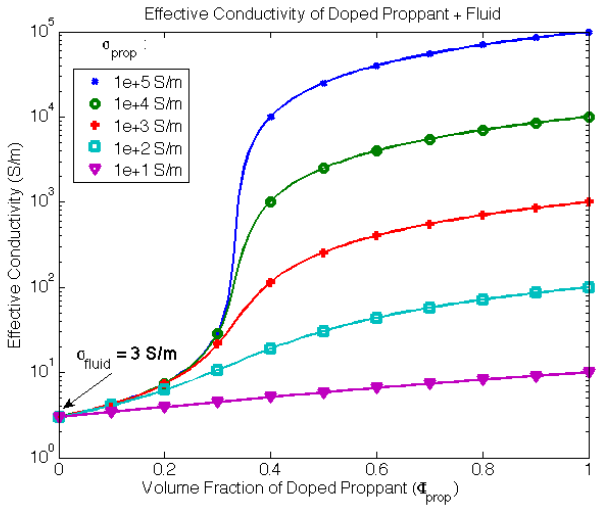

Figure 2: Effective conductivity of 5 different proppant-fluid mixtures as the volume fraction of proppant is varied.

Consider the fracture model shown in Figure 3. It consists of 10 fractures distributed along a 10 m segment of a horizontal well. Each fracture is 2.5 mm wide. The propped region of the fracture (the red region in Figure 3) extends 70 m in height and 70 m laterally. We assume that each fracture is filled with proppant and fluid, with the mixture being 50% proppant and 50% fluid, by volume. This is consistent with $350,000$ lbs of quartz sand proppant and a total volume of 60 m^3. For this example, we assume that the proppant has a conductivity similar to that of graphite, namely 10^4 S/m, and the fluid has a conductivity of 3 S/m. As shown in Figure 2, the effective conductivity of such a proppant-fluid mixture is 2500 S/m.

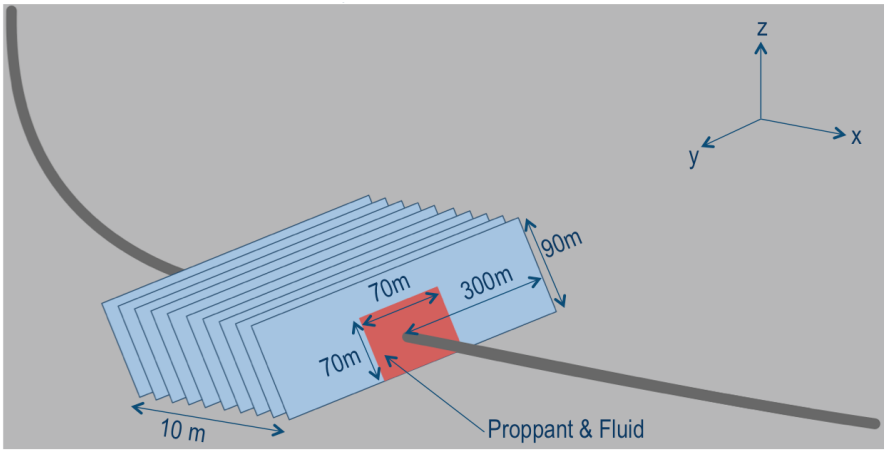

Figure 3: Example fracture model consisting of 10 fractures along a 10m segment of a horizontal well. The propped region of the fracture, in red, extends 70 m in height and 70 m laterally.

The final piece of information we require is the conductivity of the host reservoir rock. In this case, we use 0.01 S/m, consistent with a shale. With these parameters defined, we then create the effective conductivity model of our fractured reservoir.

For modelling purposes, we choose a cell size of 5 m $\times$ 5 m $\times$ 5 m, and align our mesh so that the x-axis runs parallel to the horizontal leg of the well (perpendicular to the plane of the fractures), the y-axis runs parallel to the plane of the fractures along the horizontal, and the z-axis is vertical.

In this case, we expect the effective conductivity model to consist of diagonal tensors of the form

$$\boldsymbol{\Sigma}^* = \begin{pmatrix} \sigma_x^* & & \\ & \sigma_y^* & \\ & & \sigma_z^* \end{pmatrix}.$$

with σ_x^* reflecting the behaviour of conductors in series, while σ_y^*, σ_z^* behave similar to that of conductors in parallel.

When we perform the effective conductivity calculation, we see that the conductivity model for σ_x^* does behave as a series circuit, having a value equal to that of the background, 0.01 S/m. Note that because the fractures are so thin, σ_x^* is not affected by their presence. However, for the σ_y^* and σ_z^* models, we do see the effects of the fractures, and in this case, $\sigma_y^* = \sigma_z^*$. These models are shown in Figure 4. The orange regions in the depth slice have a value of 2.5 S/m, and have

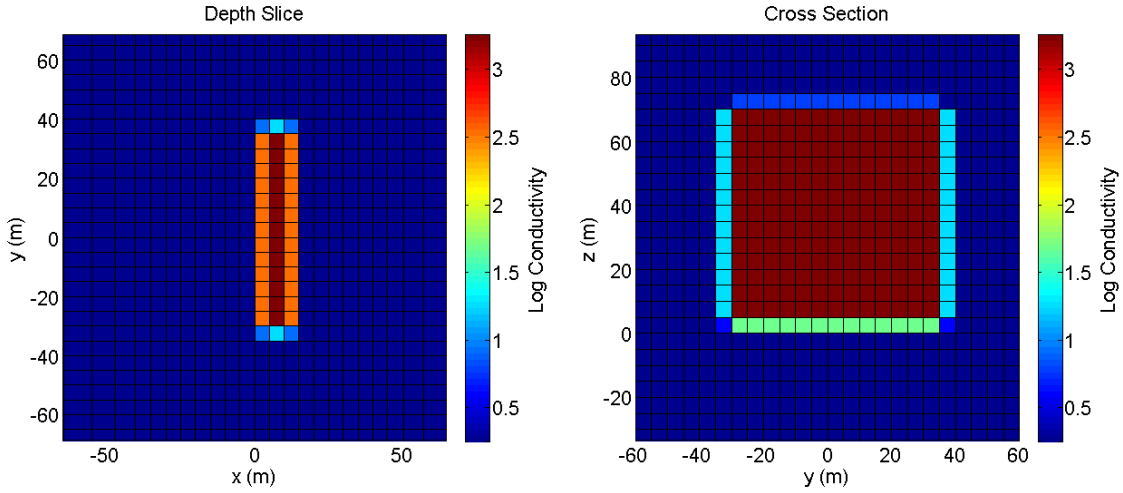

Figure 4: Depth slice (left) and cross-section (right) plots of the effective conductivity model $\sigma_y^* = \sigma_z^*$.

captured 3 of the 10 fractures, while the red region has a value of 3.4 S/m, and has captured 4 of the 10 fractures. This behaviour is consistent with our expectation that the components of the conductivity parallel to the fracture plane are more affected by its presence.

Forward Model

With the conductivity model defined, we now simulate a geophysical survey, using the set-up shown in Figure 5. A magnetic dipole transmitter is located in a horizontal well 250 m away from the treatment well, and a receiver is in a vertical well 100 m from the fracture. The transmitter has a dipole moment of 5000 Am^2, consistent with Wilt et al. (1995). The y-position of the receiver is coincident with the center of the fracture. We assume it measures 3-components of the magnetic field. For this simulation, we neglect the affects of well casing.

In Figure 6, we plot the amplitude of the x, y and z-components of the magnetic field for 5 different frequencies, ranging from 100 Hz to 1000 Hz, as measured at the receiver. The z-position of the receiver is measured relative to the base of the fracture, and is positive in the upward direction. The receiver noise floor is assumed to be 10^{-2} pT, consistent with Wilt et al. (1995). Clearly, for this survey set-up, the magnetic field response due to the presence of a fractured volume of rock is measurable in each of the 3-components, for each of the frequencies. For this survey, we see that with increasing frequency, the signal amplitude increases. However, with further increase in frequency, the signal amplitude again begins to decrease as the signal decays according to the skin depth. Also, it is important to note that low frequencies tend to be preferable in an environment

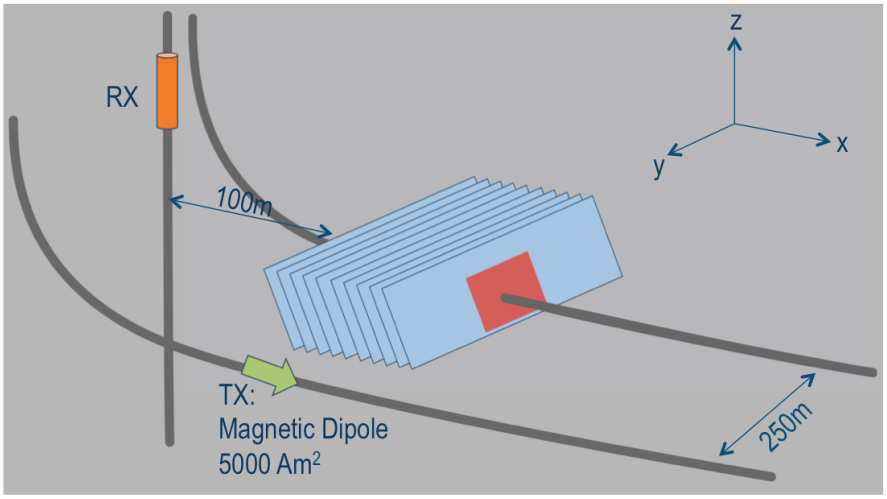

Figure 5: Schematic of the survey set-up, with a transmitter in parallel, horizontal well, and a receiver in an vertical observation well, 100 m from the fracture.

where one or both of the transmitter and receiver wells are cased with steel, as high frequencies tend to induce eddy currents in the casing, decreasing the amount of signal which penetrates the well.

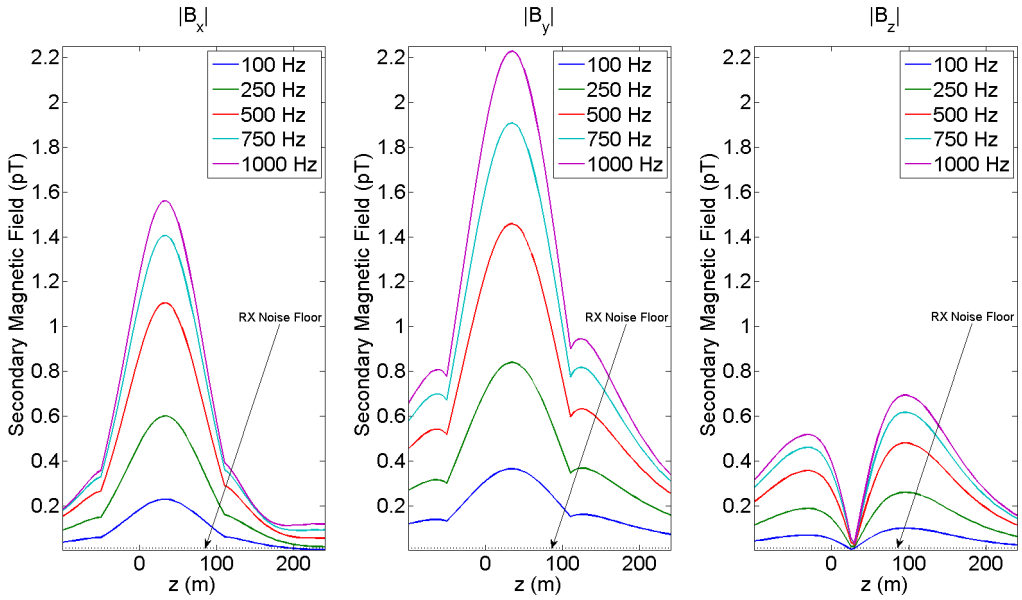

Figure 6: Amplitude of the x, y, and z-components of the magnetic field measured at the receiver.

Conclusions

By altering the physical properties of the proppant, used to keep induced fractures open, we can turn the propped region of a fracture into a geophysical target. In our example, this is accomplished by creating an electrically conductive proppant. The first step in understanding how to characterize this target is to quantify how the addition of an altered proppant affects the physical properties of the fractured reservoir. From this foundation we can construct a survey whose data are sensitive to this alteration.

Our preliminary results are encouraging in that signal obtained with current commercially available

transmitters and receivers is significantly above the noise level. In continuing work, we plan to increase the complexity of our fracture models, examine the survey design, and invert the 3D EM data to assess resolution capabilities. The ultimate goal is to ascertain whether, and under what conditions, EM imaging can provide cost effective information about the location of the proppant in a fractured reservoir.

Acknowledgments

The authors would like to thank Michael Wilt, Nestor Cuevas and Ping Zhang for their input in this project.

References

Barree, R., M. Fisher, and R. Woodroof, 2002, A Practical Guide to Hydraulic Fracture Diagnostic Technologies: Paper SPE 77442, presented at the SPE Annual Technical Conference and Exhibition held in San Antonio, Texas, 29 September - 2 October.

Berryman, J. G., and G. M. Hoversten, 2013, Modelling electrical conductivity for earth media with macroscopic fluid-filled fractures: Geophysical Prospecting, **61**, 471–493.

Britt, L. K., M. B. Smith, Z. Haddad, P. Lawrence, S. Chipperfield, and T. Hellman, 2006, Water-Fracs : We Do Need Proppant After All: Paper SPE 102227, presented at the 2006 SPE Annual Technical Conference and Exhibition held in San Antonio, Texas, USA, 24-27 September.

Bruggeman, D. A. G., 1935, The calculation of various physical constants of heterogeneous substances. I. The dielectric constants and conductivities of mixtures composed of isotropic substances: Annalen der Physik, **416**, 636–664.

Cipolla, C. L., E. P. Lolon, C. Ceramics, M. J. Mayerhofer, N. R. Warpinski, and P. Technologies, 2009, The Effect of Proppant Distribution and Un-Propped Fracture Conductivity on Well Performance in Unconventional Gas Reservoirs: Paper SPE 119368, presented at the 2009 SPE Hydraulic Fracturing Technology Conference held in The Woodlands, Texas, USA, 19-21 January.

Cipolla, C. L., and C. A. Wright, 2000, Diagnostic Techniques to Understand Hydraulic Fracturing: What? Why? and How?: SPE 59735, presented at the 2000 SPE/CERI Gas Technology Symposium held in Calgary, Alberta, Canada, 3-5 April.

Durlofsky, L. J., 2003, Upscaling of Geocellular Models for Reservoir Flow Simulation : A Review of Recent Progress: Paper presented at the 7th International Forum on Reservoir Simulation Buhl/Baden-Baden, Germany, June 23-27.

King, G. E., 2010, Thirty Years of Gas Shale Fracturing : What Have We Learned?: Paper SPE 133456, presented at the SPE Annual Technical Conference and Exhibition held in Florence, Italy, 19-22 September.

Shafiro, B., and M. Kachanov, 2000, Anisotropic effective conductivity of materials with nonrandomly oriented inclusions of diverse ellipsoidal shapes: Journal of Applied Physics, **87**, 8561–8569.

Torquato, S., 2002, Random Heterogeneous Materials: Microstructure and Macroscopic Properties: Springer.

Warpinski, N. R., 1996, Hydraulic Fracture Diagnostics: Paper SPE 39391, Journal of Petroleum Technology, 907–910.

Wilt, M. J., D. L. Alumbaugh, H. F. Morrison, a. Becker, K. H. Lee, and M. DeszczPan, 1995, Crosswell electromagnetic tomography: System design considerations and field results: Geophysics, **60**, 871–885.